

CHAPTER 5

SIMULATION OF CIRCULAR RANDOM FIELDS

5.1 Introduction

This chapter defines a new method for simulation of a circular random field (CRF) by extending the inverse cumulative distribution function (CDF) method of generating a random variable (RV). A random field (RF) is a stochastic process operating over a space. A CRF is defined as a RF containing spatially correlated circular random variables (CRV). A CRV takes random directions on a unit circle with the total probability of all possible directions distributed on the unit circle with support $[0, 2\pi)$ or equivalent support $[-\pi, \pi)$ (Chapter 1, Figure 1-1). In this chapter, the support is $[-\pi, \pi)$. Spatial correlation, which is the correlation between RVs a distance d apart, increases as distance between measurement locations decreases, i.e., rotations from the mean direction tend to be more similar as distance decreases. In the form required by the circular kriging derivation of Chapter 4, spatial correlation is defined as the mean cosine of the angle between random components of directions (non random or trend component removed) vs. distance between measurement locations. An isotropic CRF is a CRF in which spatial correlation is the same in all directions of the sample space.

This chapter is organized as follows: the background is given in Section 5.2, the new method is defined in Section 5.3, the mathematical properties are discussed in Section 5.4, qualitative evaluations are given in Section 5.5, the method is extended to any continuous RV in Section 5.6, and the chapter summary and future work are given in Section 5.7.

5.2 Background

5.2.1 Random Field

To describe a type of spatial process, Besag (1974) described the RF as a stochastic model consisting of “a finite set of sites, each site having associated with it a univariate random variable.” Mathematically, let

- The dimension of the space be $d \geq 1$ (usually $d = 2$ or 3),
- \mathbf{x} be a vector of location coordinates of a measurement location in the d -dimensional space of real numbers R^d ,
- $Y(\mathbf{x})$ be a RV at location \mathbf{x} ,
- $\mu(\mathbf{x})$ be the non random or trend component of $Y(\mathbf{x})$, which is the expected value of $Y(\mathbf{x})$ and a constant or a function of location \mathbf{x} , and
- $\varepsilon(\mathbf{x})$ be the random component of $Y(\mathbf{x})$ with mean zero.

Then, $Y(\mathbf{x}) = \mu(\mathbf{x}) + \varepsilon(\mathbf{x})$, and the RF is the set $\{Y(\mathbf{x}), \mathbf{x} \in R^d\}$.

Let $\mathbf{x}_1, \mathbf{x}_2, \dots, \mathbf{x}_n$ be a set of locations in R^d . Then, $\mathbf{Y} = (Y(\mathbf{x}_1), Y(\mathbf{x}_2), \dots, Y(\mathbf{x}_n))^T$

is a vector of RVs which map to $\mathbf{x}_1, \mathbf{x}_2, \dots, \mathbf{x}_n$ in R^d . In a spatially correlated RF, the

covariance of $Y(\mathbf{x}_i)$ and $Y(\mathbf{x}_j)$, $i, j = 1, 2, \dots, n$, is a function f which depends on the

distance and direction between RVs and decreases as the distance between RVs

increases. With E the expectation operator, the spatial covariance between $Y(\mathbf{x}_i)$ and

$Y(\mathbf{x}_j)$ in the direction of $\mathbf{x}_j - \mathbf{x}_i$ is

$$c(Y(\mathbf{x}_i), Y(\mathbf{x}_j)) \equiv c(\mathbf{x}_i, \mathbf{x}_j) = E\{(Y(\mathbf{x}_i) - \mu(\mathbf{x}_i))(Y(\mathbf{x}_j) - \mu(\mathbf{x}_j))\} = f(\mathbf{x}_j - \mathbf{x}_i). \text{ The}$$

covariance of the vector \mathbf{Y} is the symmetric and positive definite matrix

$\mathbf{C} = (c(\mathbf{x}_i, \mathbf{x}_j))$, $i, j = 1, 2, \dots, n$. In an isotropic RF, covariance is a function of distance only, i.e., $c(\mathbf{x}_i, \mathbf{x}_j) = f(\|\mathbf{x}_j - \mathbf{x}_i\|)$.

For completeness, the spatial-temporal RV with the additional coordinate of time t is introduced. $Y(\mathbf{x}, t) = \mu(\mathbf{x}, t) + \varepsilon(\mathbf{x}, t)$. Hence, the spatial-temporal RF is the set $\{Y(\mathbf{x}, t), (\mathbf{x}, t) \in \mathbb{R}^d \otimes \mathbb{R}^+\}$. In the remainder of this chapter, RFs will be considered without the coordinate t and with $d = 2$.

5.2.2 Gaussian Random Field

Worsley (2002, p. 1674) states (with notation changed for consistency in this subsection):

The definition is simple: the Gaussian random field must be multivariate Gaussian at all finite sets of points, that is, $Y(\mathbf{x}_1), \dots, Y(\mathbf{x}_n)$ must be multivariate Gaussian for all $n > 0$ and all $\mathbf{x}_i \in \mathbb{R}^d$. Since the multivariate Gaussian is specified uniquely by its mean vector and variance matrix, then the Gaussian random field is defined uniquely by its mean function $\mu(\mathbf{x}) = E\{Y(\mathbf{x})\}$ and its covariance function $c(\mathbf{x}_i, \mathbf{x}_j) = \text{cov}(Y(\mathbf{x}_i), Y(\mathbf{x}_j))$.

Let $\mathbf{y} = (y(\mathbf{x}_1), y(\mathbf{x}_2), \dots, y(\mathbf{x}_n))^T$ be a sample from $\mathbf{Y} = (Y(\mathbf{x}_1), Y(\mathbf{x}_2), \dots, Y(\mathbf{x}_n))^T$, with expectation vector $\boldsymbol{\mu} = (\mu(\mathbf{x}_1), \dots, \mu(\mathbf{x}_n))^T$ and variance-covariance matrix \mathbf{C} . Note that \mathbf{Y} (the vector of RVs) has an expectation and covariance, and that \mathbf{y} (the vector of observations) does not. Then, a Gaussian random field (GRF) is a RF in which the RVs follow the multivariate normal distribution with density

$$\frac{1}{(2\pi)^{p/2} |\mathbf{C}|^{1/2}} \exp\left[-\frac{1}{2}(\mathbf{y} - \boldsymbol{\mu})^T \mathbf{C}^{-1}(\mathbf{y} - \boldsymbol{\mu})\right].$$

Quimby (1986, p. 21) states that simulation of a GRF is accomplished by finding a factorization of the desired variance-covariance matrix \mathbf{C} . Thus, the isotropic GRF can be simulated as follows:

- 1) Generate a sequence of regular or random locations $\{\mathbf{x}_i\}$, $i = 1, 2, \dots, n$, and an equal length sequence of a standard normal RV, $\{z_i\}$, $Z \sim iid N(0, 1)$.
- 2) Pair the sequence of realizations of Z with the sequence of locations. For example, z_1 is paired with location \mathbf{x}_1 , z_2 is paired with location \mathbf{x}_2 , etc. Denote the result as $z(\mathbf{x}_1)$, $z(\mathbf{x}_2)$, etc.
- 3) With $\mathbf{x}_i = (x_{i1}, x_{i2})$, $i = 1, 2, \dots, n$, compute the pairwise distances

$$d_{ij} = \sqrt{(x_{j1} - x_{i1})^2 + (x_{j2} - x_{i2})^2}, \quad i, j = 1, 2, \dots, n,$$
- 4) With $c(d_{ij}; r, \sigma^2)$ the desired covariance function of distance d_{ij} between measurements locations, and parameters r the range and σ^2 the variance, the positive definite variance-covariance matrix $\mathbf{C} = (c_{ij})$, $i, j = 1, 2, \dots, n$ is computed with elements $c_{ij} = c(d_{ij}; r, \sigma^2)$. For example, some introductory covariance models are:

- Exponential: $c(d) = \sigma^2 \exp(-3d/r)$
- Gaussian: $c(d) = \sigma^2 \exp(-3[d/r]^2)$
- Spherical: $c(d) = \begin{cases} \sigma^2 - \sigma^2 \left(\frac{3}{2} [d/r] - \frac{1}{2} [d/r]^3 \right), & d \leq r \\ 0, & d > r. \end{cases}$

These models were derived from Bailey and Gatrell (1995, pp. 179-180).

The computed covariance values in \mathbf{C} plotted vs. the corresponding pairwise distance coincides with a plot of the desired covariance model vs. distance. Two RVs are uncorrelated at a distance equal to the range parameter of the spherical covariance model, and they are assumed to be uncorrelated at the “practical

range,” which is a distance $= 2r$ for the Gaussian model and a distance $= 3r$ for the exponential model.

- 5) The matrix \mathbf{C} is factorized such that $\mathbf{C} = \tilde{\mathbf{C}}\tilde{\mathbf{C}}^T$. Quimby (1986) states that the lower triangular method is computationally fast and numerically stable compared to the Cholesky decomposition.
- 6) With $\boldsymbol{\mu} = (\mu(\mathbf{x}_i))$, $i = 1, 2, \dots, n$, a vector of means, $\tilde{\mathbf{C}}$ a factorization of the desired variance-covariance matrix \mathbf{C} , $\mathbf{0}$ the $n \times n$ matrix of 0s, \mathbf{I} the $n \times n$ matrix with 1s in the main diagonal and 0 otherwise, and $\mathbf{Z} \sim N_n(\mathbf{0}, \Sigma = \mathbf{I})$ an n -vector of independent standard normal RVs, let $\mathbf{V} = \tilde{\mathbf{C}}\mathbf{Z} + \boldsymbol{\mu}$. Seber (1977, Theorem 1.1, Example 1.8, and Equation 1.4, pp. 8-11) proves that
 - $E\{\mathbf{V}\} = E\{\tilde{\mathbf{C}}\mathbf{Z} + \boldsymbol{\mu}\} = \tilde{\mathbf{C}}E\{\mathbf{Z}\} + \boldsymbol{\mu} = \tilde{\mathbf{C}}\mathbf{0} + \boldsymbol{\mu} = \boldsymbol{\mu}$, and
 - $\text{Cov}(\mathbf{V}) = \text{Cov}(\tilde{\mathbf{C}}\mathbf{Z} + \boldsymbol{\mu}) = \tilde{\mathbf{C}}\text{Cov}(\mathbf{Z})\tilde{\mathbf{C}}^T = \tilde{\mathbf{C}}\mathbf{I}\tilde{\mathbf{C}}^T = \tilde{\mathbf{C}}\tilde{\mathbf{C}}^T = \mathbf{C}$.
- 7) With the vector $\mathbf{z} = (z_i)$, $i = 1, 2, \dots, n$, containing the realizations of a standard normal RV Z from step 1, compute the vector $\mathbf{v} = \tilde{\mathbf{C}}\mathbf{z} + \boldsymbol{\mu}$. Pair the elements of \mathbf{v} with the \mathbf{x}_i such that v_1 is paired with location \mathbf{x}_1 , v_2 is paired with location \mathbf{x}_2 , etc. Let this be denoted as $v(\mathbf{x}_1), v(\mathbf{x}_2)$, etc. Then, the set $\{v(\mathbf{x}_i), i = 1, 2, \dots, n\}$ constitutes a simulation or realization of a GRF of mean vector $\boldsymbol{\mu}$ and variance-covariance matrix \mathbf{C} .

The function `grf` in the R package `geoR` (Ribeiro and Diggle 2001) generates simulations of GRFs for many covariance models. The function `GaussRF` in the R package `RandomFields` (Schlather 2001) generates simulations of GRFs for additional covariance models.

5.3 New Method of Generating a CRF

Figure 5-1 shows a simulation of a CRF with the von Mises CRV, parameter $\rho = .8$, which was transformed from a GRF with spherical covariance model and range $r = 10$. It was simulated using the R code in Appendices K.5 and L.3 with standardization of the realizations of the Gaussian random variable (GRV), $Z \sim N(0,1)$, to mean 0 and standard deviation 1 for demonstration. Realizations of the GRV, $z(\mathbf{x}_i), i = 1, 2, \dots, n$ with support $(-\infty, +\infty)$ are mapped to the θ with support $[-\pi, +\pi)$ as illustrated in Figure 5-2. $F_Z(z)$ the CDF of Z and $G_\theta(\theta)$ the CDF of Θ . The mapping of Z to θ is

- $z_i = -\infty$ has cumulative probability $p_i = F_Z(-\infty) = 0$ and maps to $\theta_i = G_\theta^{-1}(F_Z(-\infty)) = G_\theta^{-1}(0) = -\pi$ radians,
- $z_i = 0$ has cumulative probability $p_i = F_Z(0) = 0.5$ and maps to $\theta_i = G_\theta^{-1}(F_Z(0)) = G_\theta^{-1}(0.5) = 0$ radians,
- $z_i = +\infty$ has cumulative probability $p_i = F_Z(+\infty) = 1$ and maps to $\theta_i = G_\theta^{-1}(F_Z(+\infty)) = G_\theta^{-1}(1) = +\pi$ radians.

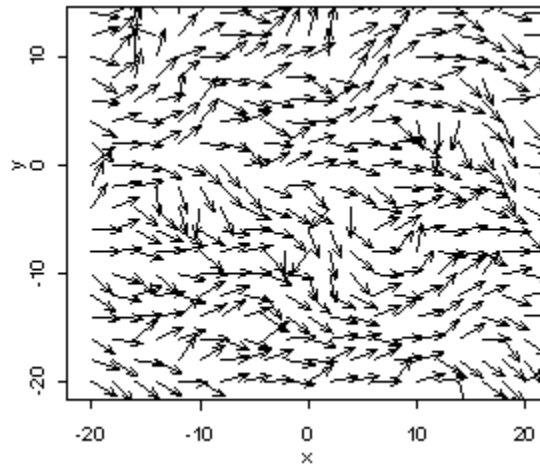


Figure 5-1. Simulated Sample of a von Mises CRF, $\rho = 0.8$, Range $r = 10$.

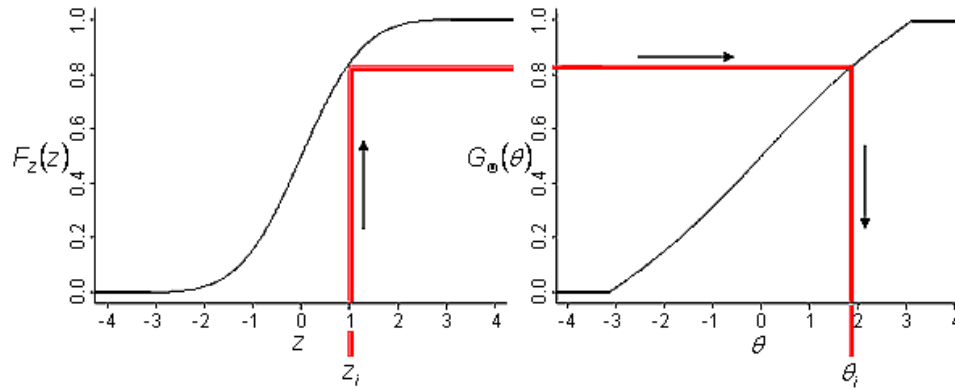


Figure 5-2. Mapping a GRV to a CRV via the CDFs F_Z and G_Θ . Direction of Θ is expressed in radian units.

A CRF may be simulated as follows:

- 1) Generate a GRF with the desired covariance model and variance $\sigma^2 = 1$. For visualization of a CRF with closer fit to the desired circular distribution, the observations $z(\mathbf{x}_i), i = 1, 2, \dots, n$ may be standardized to mean 0 and standard deviation 1. Figure 5-3 shows the standardized sample of the GRF with spherical covariance model, range $r = 10$, corresponding to Figure 5-1. Standardization should not be applied for simulation, analysis, or testing purposes as it produces undesirable effects (Subsection 5.4.4), but it may be used to obtain a single realization of an almost perfect CRF. Figure 5-3 was constructed with the R code in Appendices K.5 and L.4.

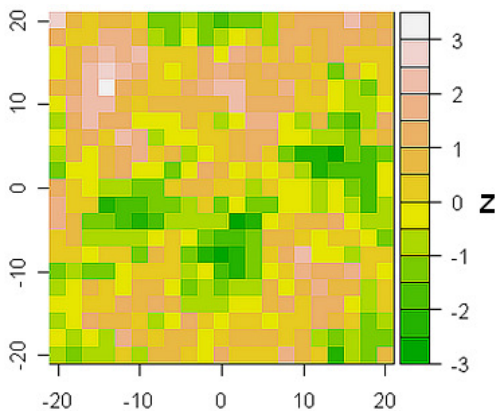


Figure 5-3. Simulated GRF with Spherical Covariance Model and Range $r = 10$ Corresponding to Figure 5-1.

- 2) For each realization $z(\mathbf{x}_i)$, $i = 1, 2, \dots, n$, compute the corresponding cumulative probability $p_i = F_Z(z(\mathbf{x}_i))$.
- 3) For the desired CRV Θ with support $[-\pi, +\pi)$ in Table 5-1, compute the inverse CDF $\theta_i = G_{\Theta}^{-1}\{F_Z(z(\mathbf{x}_i))\}$ per Table 5-2. Table 5-1 PDFs are derived in Appendix G, and Table 5-2 CDFs are derived in Appendices G and H, Equations (G.1) to (G.4), and (H.6). Note that, with exception to the triangular distribution, the PDFs of the selected distributions for support $[-\pi, +\pi)$ are identical to the PDFs for support $[0, +2\pi)$ (Chapter 3, Table 3-1).
 - For the uniform CRV, the exact inverse CDF is $\theta_i = -\pi + 2\pi p_i$.
 - For the triangular CRV, θ_i is computed by applying the quadratic solution of Appendix I, Equations (I.2), (I.3), and (I.4).
 - For CDFs containing trigonometric functions, e.g., the cardioid, von Mises, and wrapped Cauchy distributions (Table 5-2), the inverse CDF does not have a closed form. For CDFs containing trigonometric functions,
 - a) Compute a table of the desired circular CDF per Table 5-2 using a sequence of θ from $-\pi$ to π .
 - b) Interpolate the θ_i on the table of the circular CDF at p_i . Let p_L and p_U be the lower and upper cumulative probabilities bounding $p_i = F_Z(z(\mathbf{x}_i))$, and θ_L and θ_U be the corresponding directions in radians in $[-\pi, +\pi)$.
 Then, $\theta_i = \theta_L + \frac{p_i - p_L}{p_U - p_L}(\theta_U - \theta_L)$. The R implementation is given in the last page of Section K.5, Appendix K.

Table 5-1. Circular Probability Distributions in R Package CircSpatial, $\mu = 0$, $-\pi \leq \theta < \pi$ Radians. Circular density is plotted as the length of radial between black filled unit circle and outer curve.

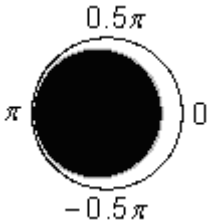
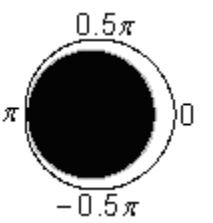
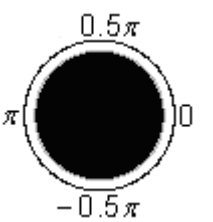
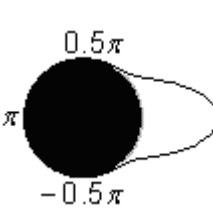
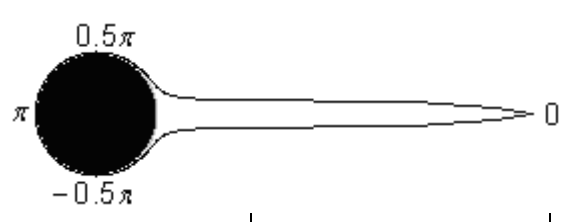
Name of Distribution	Circular PDF Plot	Circular PDF Function	Range of Parameter ρ	Value of ρ in PDF Plot
Cardioid		$\frac{1}{2\pi} [1 + 2\rho \cos(\theta)]$	$\rho = \text{mean resultant length,}$ $0 < \rho \leq 0.5$	$\rho = 0.95 \times 0.5$
Triangular		$\frac{4 - \pi^2 \rho + 2\pi \rho \delta}{8\pi}$ $\delta = \pi + \theta, -\pi \leq \theta < 0$ $\delta = \pi - \theta, 0 \leq \theta < \pi$	$0 < \rho \leq \frac{4}{\pi^2}$	$\rho = .95 \times \frac{4}{\pi^2}$
Uniform		$\frac{1}{2\pi}$	NA	NA
von Mises		$\frac{\exp(\kappa \cos(\theta))}{2\pi \sum_{j=0}^{\infty} \left(\frac{\kappa}{2}\right)^{2j} \left(\frac{1}{j!}\right)^2}$	$\kappa = \text{concentration,}$ $0 < \kappa < \infty$	$\kappa = 10.2696$ equivalent to $\rho = .95$
Wrapped Cauchy		$\frac{1}{2\pi} \frac{1 - \rho^2}{1 + \rho^2 - 2\rho \cos(\theta)}$	$0 < \rho < 1$	$\rho = 0.95 \times 1$

Table 5-2. CDFs and Inverse CDFs for Circular Distributions, $\mu = 0, -\pi \leq \theta < \pi$ Radians.

Distribution	CDF	Inverse CDF
Cardioid	$\frac{\theta + \pi + 2\rho \sin(\theta)}{2\pi}$	Interpolate CDF
Triangular	$+\frac{\rho}{8}\theta^2 + \frac{4+\pi^2\rho}{8\pi}\theta + \frac{1}{2}, -\pi \leq \theta < 0$ $-\frac{\rho}{8}\theta^2 + \frac{4+\pi^2\rho}{8\pi}\theta + \frac{1}{2}, 0 \leq \theta < \pi$	Solution in Appendix I
Uniform	$\frac{\theta + \pi}{2\pi}$	$\theta_i = -\pi + 2\pi F_Z(z(\mathbf{x}_i))$
von Mises	$\int_{-\pi}^{\theta} \frac{\exp(\kappa \cos(\phi))}{2\pi \sum_{j=0}^{\infty} \left(\frac{\kappa}{2}\right)^{2j} \left(\frac{1}{j!}\right)^2} d\phi$	Interpolate CDF
Wrapped Cauchy	$.5 - \frac{1}{2\pi} \cos^{-1}\left(\frac{(1+\rho^2)\cos(\theta) - 2\rho}{1+\rho^2 - 2\rho\cos(\theta)}\right), -\pi \leq \theta < 0$ $.5 + \frac{1}{2\pi} \cos^{-1}\left(\frac{(1+\rho^2)\cos(\theta) - 2\rho}{1+\rho^2 - 2\rho\cos(\theta)}\right), 0 \leq \theta < \pi$	Interpolate CDF

- 4) Let the pair (\mathbf{x}_i, θ_i) be denoted $\theta(\mathbf{x}_i)$. Then, the set $\{\theta(\mathbf{x}_i), i = 1, \dots, n\}$ is a simulation of the desired CRF. The function `SimulateCRF` in the R package `CircSpatial` (Appendix J, Section J.2) generates CRFs for the circular probability distributions in Table 5-1.

5.4 Mathematical Properties of the CRF

In the following subsections, the distributional and spatial properties of the circular-spatial data produced by the method of Section 5.3 will be discussed.

5.4.1 Distributional Properties of the CRF

Let Z be a continuous RV with a CDF F_Z , and define the random variable V as $V = F_Z(Z)$. Then, as shown by the CDF method in many textbooks in mathematical statistics (Rice 1995, p. 60), $V = F_Z(Z) \sim U(0,1)$, i.e., V is uniformly distributed. Also, as shown by the inverse CDF method in many textbooks in mathematical statistics (Rice 1995, p. 61), the distribution of Z can be generated by the inverse transformation $Z = F_Z^{-1}(V)$. This is a popular method for the generation of a random variable when F^{-1} is known in closed form and fast to calculate.

Now let Z be a GRV of a GRF, and $G_\Theta(\theta)$ be the CDF of the desired CRV Θ . By the CDF method, $F_Z(Z) \sim U(0,1)$, and by the inverse CDF method,

$$G_\Theta^{-1}(F_Z(Z)) \sim G_\Theta. \quad (5.1)$$

This is an extension of the inverse CDF method.

Given that a simulated GRF is a set of realizations of a GRV, it has a corresponding sample the uniform distribution equal to the cumulative probabilities of the realizations of the GRV. When this sample from the uniform distribution is input to the circular inverse CDF, the result is a sample from the desired circular distribution G_Θ .

5.4.2 Spatial Properties of the CRF

Let $\Theta(\mathbf{x})$ be a CRV at the location \mathbf{x} in 2-dimensional real space R^2 , $\mu(\mathbf{x})$ be the non random or trend component of $\Theta(\mathbf{x})$, which is the expected value of $\Theta(\mathbf{x})$ and a constant or a function of location, and $\varepsilon(\mathbf{x})$ be the random component of $\Theta(\mathbf{x})$, which follows a circular probability distribution. The parameters of the circular probability distribution, which are based on the unit vector form of the CRV, are the mean resultant direction μ , and the mean resultant length ρ , which is a measure of concentration

about the μ (Chapter 3, Subsection 3.3.1). Then, $\Theta(\mathbf{x}) = \mu(\mathbf{x}) + \varepsilon(\mathbf{x})$, and the CRF is the set $\{\Theta(\mathbf{x}), \mathbf{x} \in R^2\}$.

As required by the circular kriging derivation of Chapter 4, circular-spatial correlation is expressed as the mean cosine of the angle between random components of direction $\zeta(d)$ as a function of the distance d between measurement locations (isotropic CRF). Let D_{ij} (Chapter 3, Figure 3-3) be the angle or circular distance between the random components of direction of observations i and j , and n the number of observations of a sample,

$$D_{ij} = (\Theta(\mathbf{x}_j) - \mu(\mathbf{x}_j)) - (\Theta(\mathbf{x}_i) - \mu(\mathbf{x}_i)) = \varepsilon(\mathbf{x}_j) - \varepsilon(\mathbf{x}_i), \quad i, j = 1, 2, \dots, n, \text{ and}$$

$$\zeta(d) = E\{\cos(D_{ij})\} = E\{\cos(\varepsilon(\mathbf{x}_j) - \varepsilon(\mathbf{x}_i))\}, \quad \|\mathbf{x}_j - \mathbf{x}_i\| = d.$$

5.4.2.1 Mean Cosine at Distance Zero

When the distance between measurement locations goes to zero, the mean cosine $\zeta(0)$ is taken of the angle between a CRV and itself, i.e., $D_{ij} \xrightarrow{\mathbf{x}_j \rightarrow \mathbf{x}_i} D_{ii} \equiv 0 \Rightarrow E\{\cos(D_{ii})\} = E\{\cos(0)\} = 1$. Thus, the mean cosine at zero distance is one, which is the maximum. The mean cosine is observed to approach one as distance between measurement locations approaches zero.

Measurement error may cause measurements which are located close together to be more different, resulting in a cosineogram with a mean cosine less than one for distances close to zero. This reduction in the mean cosine is called the nugget as in the kriging of linear RVs.

5.4.2.2 Mean Cosine at Distances Where CRV Are Spatially Correlated

In a GRF with spatial correlation, observations of the GRV tend to be increasingly similar as the distance between measurement locations decreases. Because the CDF of the GRV Z is a one to one and strictly increasing function, the corresponding cumulative probabilities of the GRV will also tend to be increasingly similar. Thus, spatially correlated GRV map to spatially correlated cumulative probabilities. Conversely, by the extended inverse CDF method of Section 5.3, the transformation (5.1) of spatially correlated cumulative probabilities via the one to one and strictly increasing circular inverse CDF results in spatially correlated CRV. The measurement location coordinates are not transformed. Hence, the set of untransformed spatial coordinates of the GRF and the corresponding computed CRV constitute a simulated CRF.

Figure 5-4 contains two variograms and one cosineogram (Chapter 3). In the kriging of a linear RV, with σ^2 the variance of the RV, r the scale parameter, and $c(d, r)$ the covariance model dependent on the distance d between measurement locations, spatial dependence is expressed as the semivariance $\gamma(d) = \sigma^2 - c(d, r)$. The variogram is a plot of $\hat{\gamma}$ vs. d . It is a robust alternative to the empirical covariance. For the cosineogram, spatial correlation is expressed as the mean cosine of the angle between random components of directions. Where the CRV are uncorrelated, the mean cosine and the semivariance form a plateau, which is called the sill.

Figure 5-4 was constructed using the R code in Appendices K.4 and L.5 with standardization of the GRF of spherical covariance and range $r = 10$, and for a von Mises CRF of $\rho = 0.8$.

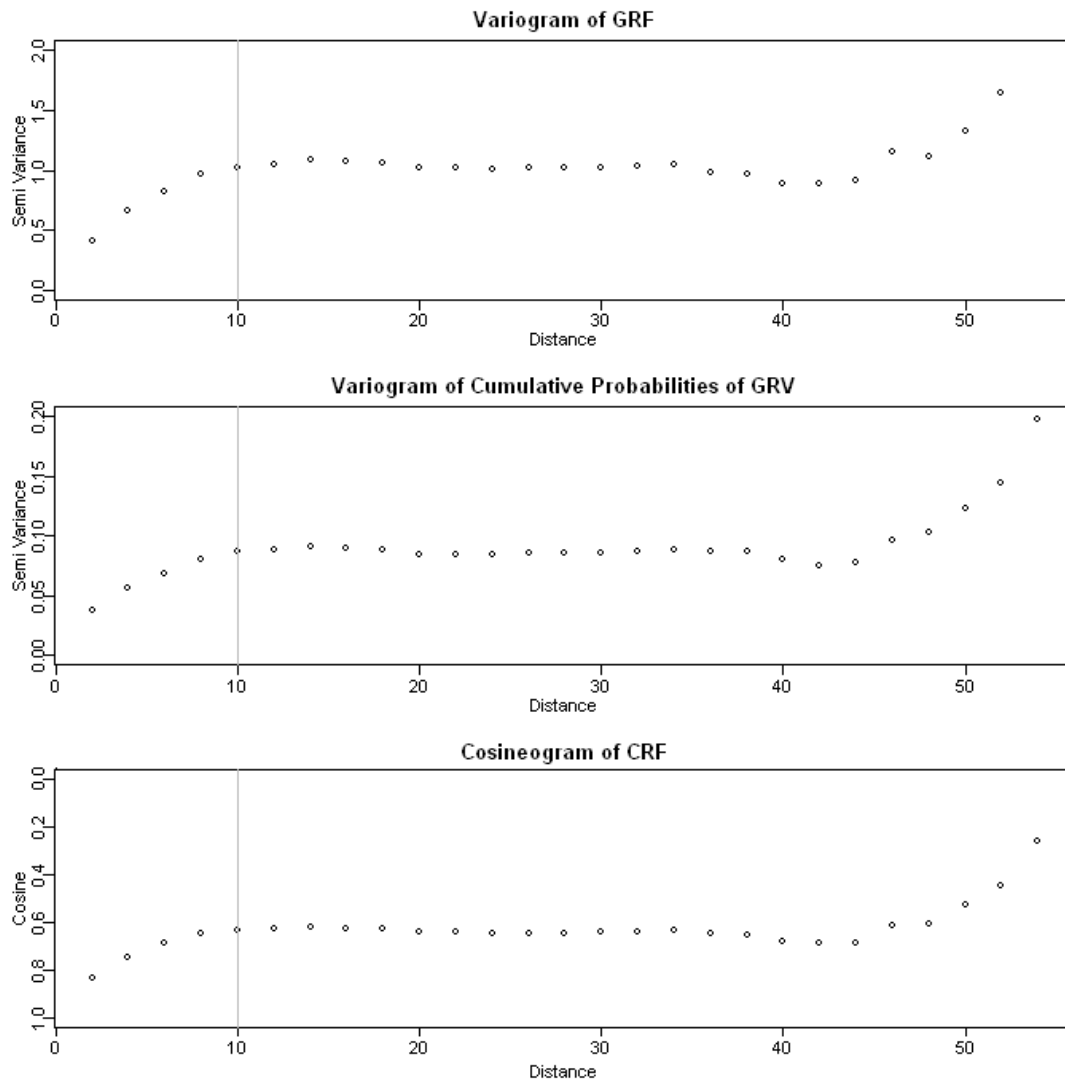


Figure 5-4. Similar Shapes of Variograms and Inverted Cosineogram Reflect Transformations of the Spatial Correlation of the GRF. This figure corresponds to Figures 5-1 and 5-3.

The cosineogram, an analogue of the covariogram (an inverted variogram), was inverted vertically to compare its shape to the shapes of the corresponding variograms. Note that the cosine axis labels are reversed in the bottom plot. The grey vertical lines are plotted at the value of the range input parameter of the GRF covariance model.

Figure 5-4, which corresponds to Figures 5-1 and 5-3, shows that the variogram of the sample of the GRF, the variogram of the cumulative probabilities of the

realizations of the GRV, and the inverted cosineogram of the CRF, are similar in shape. Hence, the computed CRVs have spatial correlation resembling, but not identical to the spatial correlation of the cumulative probabilities and of the GRF. How may the circular-spatial correlation be characterized?

The mean cosine function of distance is implicit in the relationship between the GRF covariance model and the simulated CRV. Let's build up an expression of that relationship. With (x_i, y_i) and (x_j, y_j) the coordinates of two measurement locations, the distance from location (x_i, y_i) to location (x_j, y_j) is $d_{ij} = \sqrt{(x_i - x_j)^2 + (y_i - y_j)^2}$. Next, with $c(d_{ij})$ the covariance model of the GRF, E the expectation operator, and $Z(x_i, y_i)$ and $Z(x_j, y_j)$ mean 0 variance 1 GRVs of the GRF at (x_i, y_i) and (x_j, y_j) , respectively, the covariance function of distance is

$$\begin{aligned} c(d_{ij}) &= c\left(\sqrt{(x_i - x_j)^2 + (y_i - y_j)^2}\right) \\ &= E\{Z(x_i, y_i) Z(x_j, y_j)\} - \underbrace{E\{Z(x_i, y_i)\}}_0 \underbrace{E\{Z(x_j, y_j)\}}_0 \\ &= E\{Z(x_i, y_i) Z(x_j, y_j)\} \end{aligned}$$

Next, with F_Z the CDF of the GRV Z , and G_Θ the CDF of the CRV Θ , apply the method of simulating a CRF (Section 5.3). Hence, $\Theta(x_i, y_i) = G_\Theta^{-1}(F_Z(Z(x_i, y_i)))$ and

$$\Theta(x_j, y_j) = G_\Theta^{-1}(F_Z(Z(x_j, y_j))). \text{ Conversely,}$$

$$F_Z^{-1}(G_\Theta(\Theta(x_i, y_i))) = F_Z^{-1}(G_\Theta(G_\Theta^{-1}(F_Z(Z(x_i, y_i)))))) = Z(x_i, y_i) \text{ and likewise}$$

$$F_Z^{-1}(G_\Theta(\Theta(x_j, y_j))) = Z(x_j, y_j). \text{ Substituting for } Z(x_i, y_i) \text{ and } Z(x_j, y_j) \text{ in the covariance}$$

expression, the expression of the general relationship is

$$c\left(\sqrt{(x_i - x_j)^2 + (y_i - y_j)^2}\right) = E\left\{ \underbrace{F_Z^{-1}(G_\Theta(\Theta(x_i, y_i)))}_{Z(x_i, y_i)} \underbrace{F_Z^{-1}(G_\Theta(\Theta(x_j, y_j)))}_{Z(x_j, y_j)} \right\}.$$

For a specific example, let the covariance function be spherical (Subsection 5.2.2, step 4), point 3) with range r and $\sigma^2 = 1$. Then,

$$c(d_{ij}) = \begin{cases} 1 - 1.5 \frac{d_{ij}}{r} + 0.5 \left(\frac{d_{ij}}{r} \right)^3, & d_{ij} \leq r \\ 0, & d_{ij} > r. \end{cases}$$

Now let the CRV of the CRF mapping from the GRF have a cardioid circular CDF with parameter ρ (Table 5-2). Then, $G_\Theta(\Theta(x_i, y_i)) = \frac{\Theta(x_i, y_i) + \pi + 2\rho \sin(\Theta(x_i, y_i))}{2\pi}$. Hence, the complete expression of the relationship between the spherical covariance of the GRF and the cardioid CRV of the CRF is

$$\begin{aligned} & E \left\{ F_Z^{-1} \left(\frac{\Theta(x_i, y_i) + \pi + 2\rho \sin(\Theta(x_i, y_i))}{2\pi} \right) F_Z^{-1} \left(\frac{\Theta(x_j, y_j) + \pi + 2\rho \sin(\Theta(x_j, y_j))}{2\pi} \right) \right\} \\ &= \begin{cases} 1 - 1.5 \frac{d_{ij}}{r} + 0.5 \left(\frac{d_{ij}}{r} \right)^3, & d_{ij} \leq r \\ 0, & d_{ij} > r. \end{cases} \end{aligned}$$

The problem is then to transform this nonclosed form relationship into an expression of the mean cosine of the angle between CRV vs. distance $\varsigma(d_{ij})$ and the parameters r and ρ .

As an alternative to the derivation of an approximating expression characterizing the mean cosine vs. distance produced by the method of Section 5.3, the cosine curve may be described by an approximating covariance model of a GRF with translation and scaling (Chapter 3, Subsection 3.6.2). With ρ the mean resultant length of the circular probability distribution, $0 \leq \rho < 1$, n_g the nugget, $0 \leq n_g < 1 - \rho^2$, and $c(d)$ the covariance function of distance d from linear kriging with a maximum value of one,

the cosine model is

$$\varsigma(d) = \begin{cases} 1, & d = 0 \\ \rho^2 + (1 - n_g - \rho^2)c(d), & d > 0. \end{cases} \quad (5.2)$$

Hence, the mean cosine is 1 at zero distance, 1 minus the nugget at distances close to 0, greater than ρ^2 and less than 1 minus the nugget at distances where CRV are correlated, and ρ^2 at distances where CRV are uncorrelated (Chapter 3, Equation (3.11)). Some introductory cosine models were given in Chapter 3, Subsection 3.6.2, and additional models are tabulated for a wide range of conditions in Appendix M, Section M.5.

Even though cosine models are not fully specified in the CRF domain as closed form expressions, but as transformations from the GRF domain, the cosine models acquire practical meaning as they apply to real world data (Chapter 3, Section 3.7, Figure 3-13).

5.4.2.3 Mean Cosine at Distances Where CRV Are Uncorrelated

Applying the method of Section 5.3, the location coordinates of the GRV are untransformed. At distances at which the GRV are uncorrelated, the transformations of the GRV are also uncorrelated. Thus, the corresponding cumulative probabilities $F_Z(z(\mathbf{x}_i))$ and simulated CRV $\theta(\mathbf{x}_i) = G_{\Theta}^{-1}(F_Z(z(\mathbf{x}_i)))$ are uncorrelated at distances where the GRV are uncorrelated. Hence, the distance at which the computed CRV are uncorrelated equals the distance at which the GRV are uncorrelated. In the example of Figure 5-4 with spherical covariance, the distance at which RVs are uncorrelated is approximately the range $r = 10$.

In Chapter 3, Section 3.3, the theoretical sill, which is the expectation of the cosine of the angle between independent random components of the CRVs was derived. The sill is equal to the square of the mean resultant length of the circular probability distribution. In Chapter 3, Section 3.4, it was determined that the vector resultant mean length is the parameter ρ of the circular distributions examined, which are the cardioid, triangular, uniform ($\rho = 0$), von Mises, and wrapped Cauchy distributions. Hence, the sill is ρ^2 . Hence, the mean cosine will be ρ^2 at distances at which the GRV are uncorrelated.

5.4.3 Overfitting Improves Fit of the Output CRV to the Desired CRV

The QQ (quantile-quantile) plot is a graphical method in which data are plotted against the expected values of a comparison distribution. The QQ plot shows a linear pattern when the data come from the comparison distribution. In Section 5.3, it is stated that the realizations of the GRV can be standardized to mean 0 and standard deviation 1. This was motivated by the observation that the variation in the mean and standard deviation of the GRV transforms to variation in the mean resultant direction and the mean resultant length, respectively, of the output CRF. Hence, standardizing the realizations of the GRV results in a closer fit of the output CRV to the desired CRV. The resulting CRF simulation is over fitted, but useful to demonstrate or visualize a closely fitting simulation.

Figure 5-5 was constructed using the R code in Appendices K.13 and L.6. For each of 30 simulations of a GRF (spherical covariance, range=10, variance=1, with standardization of the realizations of the GRV), the point coordinates of the QQ standard normal plot and the QQ circular uniform plot were accumulated separately. At the conclusion of the simulations, the point density was computed for each set of points.

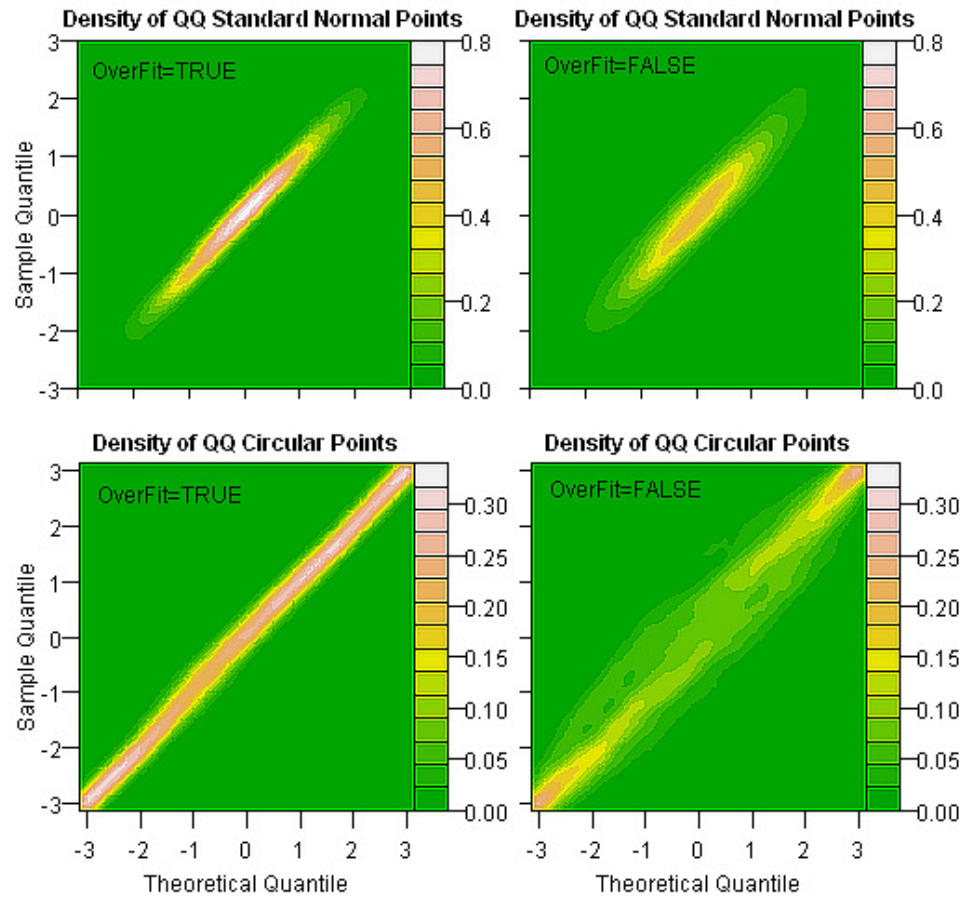


Figure 5-5. Standardization of the GRV Increases Fit of the GRV and the CRV. The uniform CRV was transformed from a GRF with spherical covariance and range=10. Circular quantiles are expressed in radian units. QQ density plots for other circular distributions with ρ at mid point of the parameter range allowed by the distribution showed results similar to Figure 5-5.

The same simulations were repeated without standardization by setting the seed of the random number generating process to the seed value prior to the first set of simulations. Again, the QQ plot points were separately accumulated, and the point densities computed for each of the two sets of points. In Figure 5-5, point density is shown as color. The greater the density about a straight line, the closer the realizations of a RV are to the comparison distribution. In the left plots, realizations of the GRV are standardized prior to transformation to the CRV (OverFit = TRUE in R package CircSpatial function SimulateCRF, Appendix J, Section J.2). In the right plots, realizations of the GRV are not standardized (OverFit = FALSE). The point mass in the left plots is more concentrated along the straight line of equality than the point mass in the right plots. This indicates that standardization results in a closer fit to the desired distributions.

Figure 5-6, which was constructed using the R code in Appendices K.13 and L.7, demonstrates the effect of decreasing ρ without standardization of the GRV on the fit of a CRV. The triangular CRV (Table 5-1) was arbitrarily selected. As ρ is decreased, dispersal of the QQ point mass increases. In the bottom plots with $\rho = 25\%$ of the maximum $(0.25 \times 4/\pi^2)$, standardization dramatically reduces dispersal of QQ point mass in the right plot. It is apparent that without standardization, the variability of the fit, which is indicated by the QQ point mass dispersal, increases as ρ decreases. This does not mean in general that standardization is desirable. In the next section, the undesirable effects of standardization are discussed.

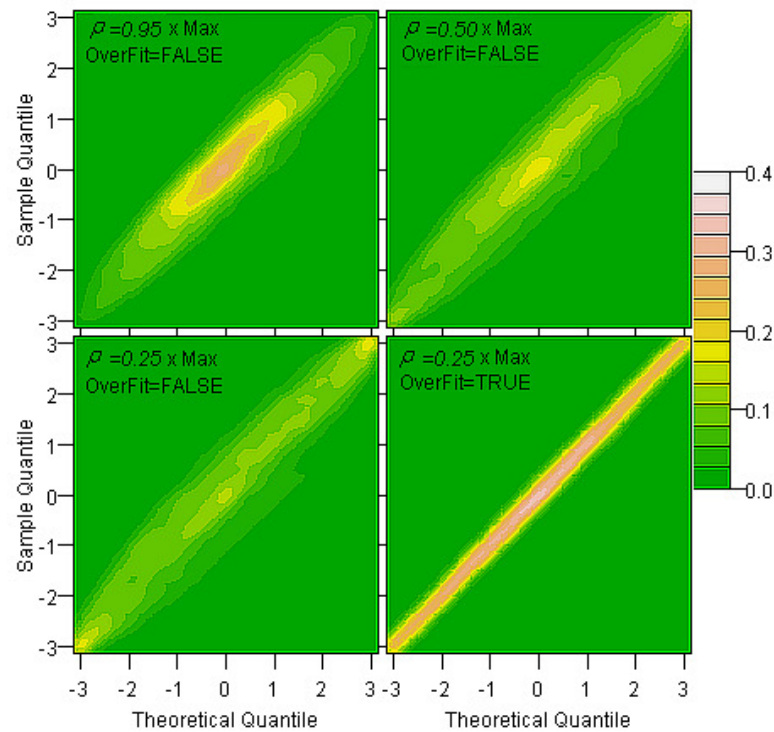


Figure 5-6. Variability of Fit of the Simulated Triangular CRV Increases as ρ Decreases. Circular quantiles are expressed in radian units.

5.4.4 Overfitting Has Unwanted Effects

Figure 5-7 was constructed by fitting 400 variograms made from the 400 simulations of a GRF with spherical covariance, range=10, variance=1. In the first set of simulations, realizations of the GRV were standardized. The sequence of simulations was repeated without standardization by setting the seed of the random number generating process to the seed value prior to the first set of simulations. The right plot without standardization has the correct variance of 1 at distance = 10. The left plot with standardization has a biased variance at distance = 10. If variation in the center and scale of the GRV is eliminated by standardization, everything that is derived from the CRF is altered. If a test were constructed based on simulations with standardization, a simulation without standardization would more likely appear as unusual and be rejected in a test of hypothesis, inflating the type 1 error.

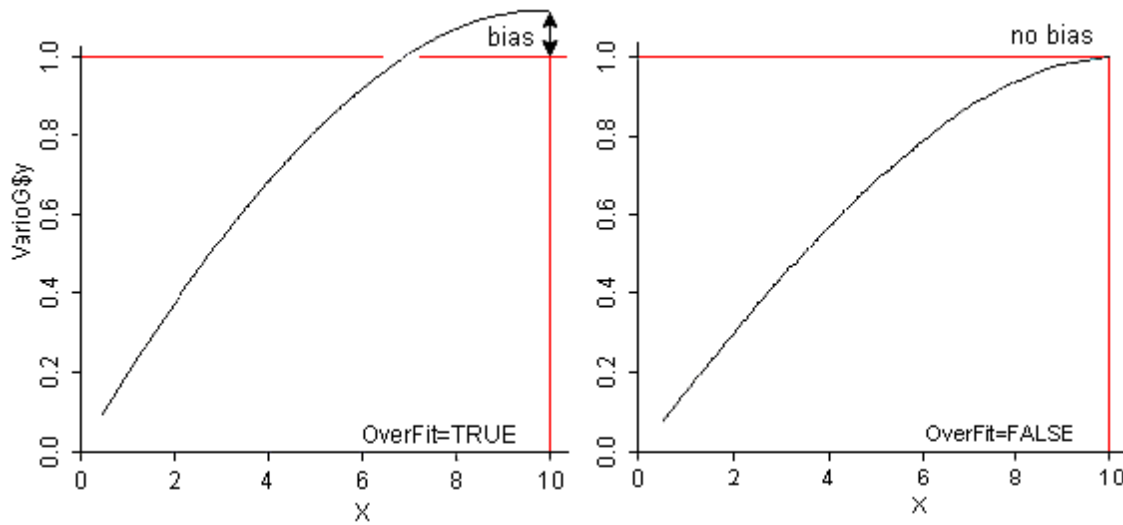


Figure 5-7. Standardization of the GRV Biases the GRF Covariance. The plots are averages of variograms (inverted covariance) of GRF with spherical covariance, range=10, and variance=1.

In summary, standardization is suitable for demonstration of a CRF with closer fit for visualization, but should not be used for the purposes such as simulation, analysis, and testing.

5.5 Qualitative Evaluations of Method of Simulating a CRF

5.5.1 Review

In this section, QQ plots will be used to show agreement with the desired probability distributions, and the variogram and the cosineogram will be used to show agreement with the desired spatial properties. In the kriging of a linear RV, with σ^2 the variance of the RV and $c(d,r)$ the covariance model with range (scale) parameter r and dependent on the distance d between measurement locations, spatial dependence is expressed as the semivariance $\gamma(d) = \sigma^2 - c(d,r)$. The variogram is a plot of $\hat{\gamma}$ vs. d . It is a robust alternative to the empirical covariance. For the cosineogram, spatial correlation is expressed as the mean cosine of the angle between random components

of directions. Where the CRV are uncorrelated, the mean cosine and the semivariance form a plateau, which is called the sill.

5.5.2 Construction of Figure 5-8

Figure 5-8 was computed using the R code in Appendices K.6 and L.8. The von Mises CRF, $\rho = 0.8$, was transformed from a realization of a GRF with spherical covariance, range $r = 10$, with standardization of the realizations of the GRV to 0 mean and standard deviation 1 for close fit. Figure 5-8, which closely corresponds with and is based on the same data as Figures 5-1, 5-3, and 5-4, provides qualitative evaluations of the standardized GRF and the CRF.

Per the R function “ppoints”, with k the index of the order statistic, n the number of observations, and $c_n = \begin{cases} 3/8, & n \leq 10 \\ 1/2, & n > 10 \end{cases}$, the theoretical quantile of the QQ plots is computed based on the corresponding cumulative probability $= (k - c_n)/(n + 1 - 2c_n)$.

5.5.3 Evaluations

In the QQ plots on the left of Figure 5-8, the degree of fit is indicated by proximity of the plotted curve to the straight line of equality through the origin. Although the QQ plot can show clear departures from the comparison distribution as a structured deviation from a straight line, minor departures may be indistinguishable from the typical variation of sampling from the comparison distribution.

The upper left plot is the QQ Standard Normal plot of the realizations of the GRV of the GRF. The blue line through the origin represents the standard normal probability distribution. The standardized realizations of the GRV (black curve) display a high degree of fit to the standard normal distribution. The GRV is over fit as described in Subsection 5.4.3.

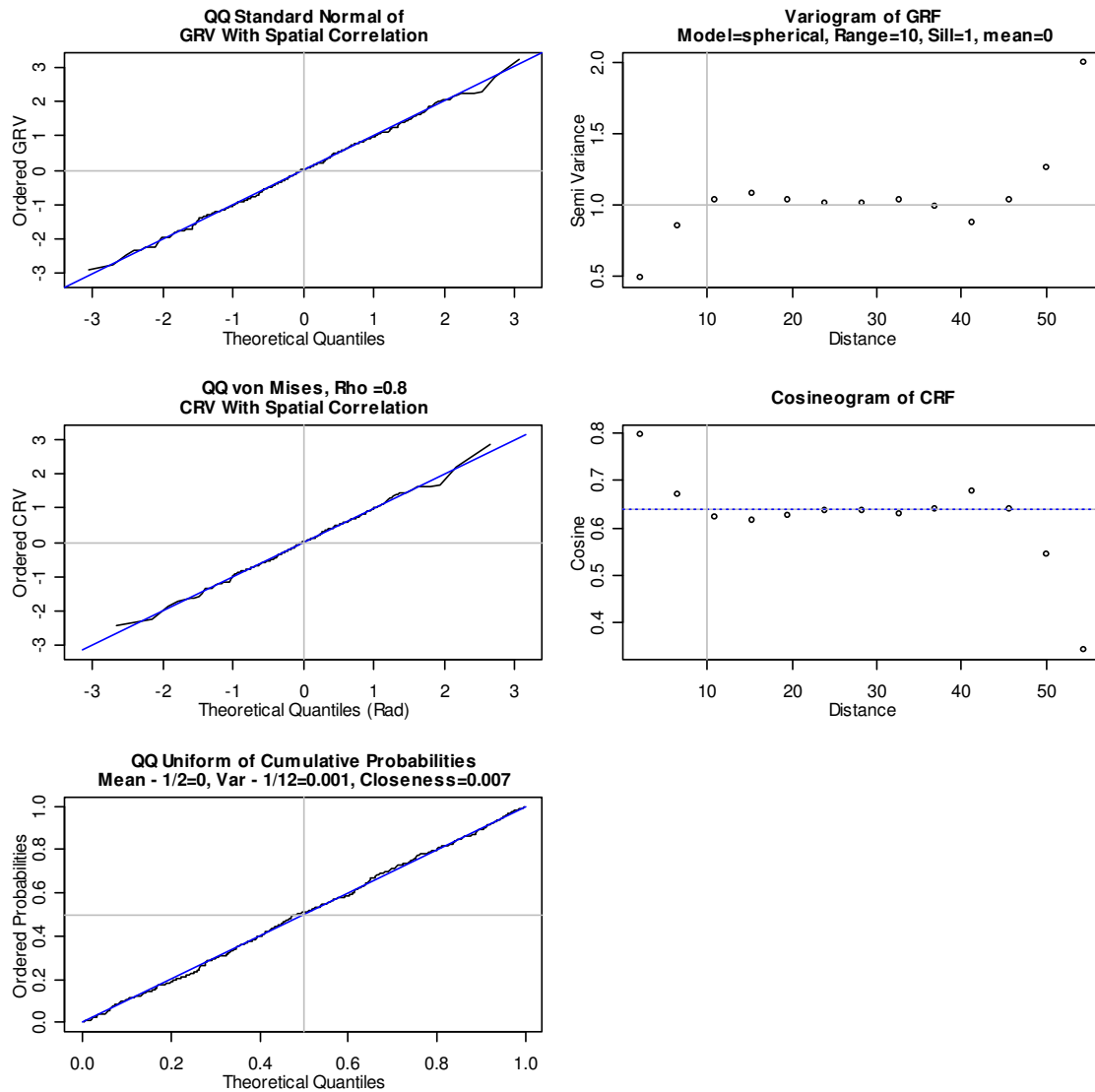


Figure 5-8. Evaluation of a von Mises CRF, $\rho = 0.8$, Overfit, Range $r = 10$. The CRF, which was transformed from a GRF with spherical covariance corresponds to Figures 5-1, 5-3, and 5-4. The QQ standard normal (top left) plot, the QQ von Mises plot (middle left), and the QQ uniform plot (bottom left) plots show simulations with close fits. The range of the variogram of the GRF (top right) and of the cosineogram (middle right) of the CRF match the input range 10. The square of the sample mean resultant length (blue dashed horizontal line) of the cosineogram is visually indistinguishable from ρ^2 (grey horizontal line).

The middle left plot is the QQ circular plot of the simulated CRV of the CRF.

The title is automatically generated by the input specifications for subsequent reference.

Thus, the CRF input specifications are von Mises distribution with $\rho = 0.8$. The blue line through the origin represents the desired distribution, which is the von Mises $\rho = 0.8$. The simulated CRV (black curve) displays a high degree of fit to the desired distribution.

The bottom left plot is the QQ Uniform plot of the cumulative probabilities of the realizations of the GRVs. The QQ Uniform plot displays a high degree of fit to the uniform distribution. According to the inverse CDF method, the high degree of fit predicts a high degree of fit for the CRV. The subtitle is automatically generated with three metrics of fit for evaluation. By the CDF method, the cumulative probabilities of a RV are uniformly distributed. When $X \sim U[0,1]$, $E\{X\} = 0.5$ and $Var(X) = 1/12$. Hence, the fit of the cumulative probabilities to the uniform distribution may be measured as the mean cumulative probability minus 0.5, and as the variance of cumulative probabilities minus 1/12. Then, if the variance minus 1/12 is negative, data are more concentrated in the middle. If the difference is positive, the data are more concentrated toward the tails. The deviation of the mean from 0.5 indicates an off center condition with positive deviation indicating a shift towards higher values. Additionally, “closeness” is defined as the mean vertical distance between QQ uniform plot points and the line through the origin. Hence, zero indicates a perfect fit. These metrics provide information to assess fit.

The upper right plot is a variogram reflecting the spatial properties of the GRF.

The plot subtitle is generated by the input specifications for subsequent reference.

Hence, the GRF input specifications are spherical covariance, range = 10, sill = 1, and mean=0. The grey vertical line is located at the input range of 10 and the grey horizontal

line is located at the input sill of 1. The variogram has a sill of about 1.0 and a range of about 10 consistent with the input specifications.

The bottom right plot is the cosineogram of the simulated CRF. The shape of the cosineogram is similar to the shape of the inverted variogram (upper right plot). The grey vertical line is the input range. The cosineogram matches the range input. The grey horizontal line, which is the theoretical sill ρ^2 , is visually indistinguishable from the blue dotted horizontal line, which is the square of the sample mean resultant length r . Thus, the cosineogram sill, the theoretical sill, and the sample mean resultant length squared are all close together. Hence, these observations evidence that the CRF has the correct range and sill.

Additional examples, with ρ set to one half of the maximum (Table 5-1), with standardization of the realizations of the GRV and selected with regard for fit, are shown in Appendix C. Further examples, with ρ set to the extremes of 5% and 95% of the maximum, with and without standardization of the GRV for comparison, and generated sequentially without regard for fit, are shown in Appendix D. The spatial properties were scored, and summarized in Table D-1. The conclusion was that the QQ plots with standardization indicated a high degree of fit. Standardization of the GRF had no apparent effect on agreement of the spatial properties of a simulation with the desired spatial properties.

5.6 Extension of the Method

The extension of the inverse CDF method to the simulation of circular random fields may be applied to any continuous RV whose CDF can be computed, or whose inverse CDF exists in closed form following the method of Section 5.3.

5.7 Chapter Summary and Future Work

The CRF was defined as a RF consisting of spatially correlated CRVs. The well known inverse CDF method, i.e., the fact that the inverse CDF of the desired RV operating on a uniform RV produces the probability distribution of the desired RV, was extended to the production of a CRF. The GRV component of a GRF with spatial correlation has spatially correlated cumulative probabilities. The inverse CDF of the desired circular probability distribution operating on the spatially correlated cumulative probabilities produces a spatially correlated CRV. The combination of the computed CRV and the untransformed coordinate locations of the corresponding realizations of the GRV is a simulation of the CRF. This method is applicable to any continuous RV.

The spatial properties of the simulated CRF were discussed. The spatial correlation of circular-spatial data is expressed as the mean cosine of the angle between random components of direction observed at a distance d apart vs. d as required by the circular kriging solution of Chapter 4. These properties include:

- 1) The mean cosine at distance zero is one. A discontinuity may exist near zero due to measurement error. The size of the discontinuity is called the nugget.
- 2) The mean cosine behavior between distance zero and the distance at which RVs are uncorrelated was characterized by closely fitting shifted and scaled positive definite covariance functions from linear kriging.
- 3) The mean cosine at distances where GRV and CRV are uncorrelated is the square of the mean resultant length of the CRV component of the CRF. For the circular probability distributions examined, it is ρ^2 , with ρ the mean resultant length parameter of the CRV.

Standardization of the realizations of the GRV to mean 0 and standard deviation 1 was examined. Standardization results in bias of the GRF variance, over fitting of the desired the CRF, and inflated type 1 error in tests based on simulation of over fitted realizations. Hence, over fitting may be used for the purpose of visualization of close fit, but should not be used for simulation, testing, or analysis. Qualitative evaluations of over fitted simulations demonstrated that CRFs produced were correct. The CRV component of the CRF had a close fit to the desired circular distribution, the sill matched ρ^2 , and the similarity of shape of the inverted cosineogram and variogram indicated that the range of the output CRF matched the desired range.

Metrics of fit were introduced based on the realizations of the uniformly distributed cumulative probabilities corresponding to the realizations of the GRV. The mean vertical distance between the QQ uniform plot points and the line of perfect fit through the origin measured the overall fit of the samples of the GRV and the CRV. The mean minus 1/2 measured shift (+ upward, - downward), and the variance minus 1/12 measured departure from the variance of the uniform RV generating the GRV and the CRV (+ more spread, - more concentrated).

Future work includes: Implementation of additional circular probability distributions for simulating CRFs; analysis of how the cosine behavior of the simulated CRF relates to the input spatial covariance model of the GRF; automatic fitting of the cosine models such as in Appendix M to the cosineogram with identification of best fit; and determination of what metrics of fit would be considered a good fit.